

## RESEARCH ARTICLE

# Investigating the Steel Fiber of Waste Tires to Enhance the Properties of Concrete Ground Slabs

Afif Rahma<sup>1,\*</sup>

<sup>1</sup>Structure Department, Arab International University, Syria

**Abstract:** This research aims to demonstrate the potential and viability of investing in smooth steel fibers extracted from waste tires for concrete works such as factory ground slabs and airstrip slabs, exposed to soil–structure interaction under live loads and the reciprocal alternation between tension and compression stresses. To show this viability, samples of fiber concrete and plain concrete were prepared and tested for compression, bending, and splitting loads. The main problem was the physical stability of samples and effective coherence between the concrete and the steel fibers during loading; thus, to analyze the laboratory results and assess the impact of fibers on mechanical properties of concrete under compression load, a method has been proposed to evaluate the effective ductility of fiber concrete and to calculate “the toughness and toughness index,” taking into account the discontinuity and the physical destabilization of the sample state observed during the loading in the post-elastic stage. The analysis of the experimental results has shown satisfactory improvement in the behavior of concrete under compression and tension loads in the elastic domain, as well as a significant increase in its ductility and toughness in the plastic domain by two to four times compared to plain concrete. Likewise, this research shows that the inclusion of steel fiber enhances the mechanical properties of plain concrete by more than three times under splitting and flexure. This work resulted in its objectives where experimental tests proved the feasibility of investing in this raw material classified as a pollutant left freely in nature; on the other hand, the statistical analysis of the experimental results showed the best characteristics of fibers in terms of length, slenderness, and volume ratio to have a high range of fiber concrete for ground slab.

**Keywords:** smooth steel fibers, waste tires, ductility, effective toughness, effective toughness index compression strength, tension strength, spilling strength

## 1. Introduction

The topic of exploitation of steel fibers from the recycling of used tires in concrete mixes remains a research problem to this day, where each study confirms the profitability of this material randomly dispersed in nature. In 2022, the “Tire Industry Project for the World Business Council for Sustainable Development” asserts that one billion end-of-life tires are generated annually. The report estimates that there are currently more than 4 billion such tires in landfills and stockpiles worldwide. Similarly, the report assessment of markets for fiber and steel produced from recycling waste tires, established in 2003 by the State of California, estimates that steel fiber in the tire composition can reach 15% of its weight [1].

From an environmental point of view, Šourková and Adamcová [2] evaluated the degree of phytotoxicity caused by the long-term action of used tires exposed on landfills by analyzing chemical changes in the soil; furthermore, the detrimental effects of waste tires were thoroughly examined by Czarna-Juszkiec et al. [3], where they elucidated how this practice may impact ecosystems and human health.

The exploitation of used tires for various applications has been a prominent research topic for decades and continues to be so today. Thus, numerous studies have been conducted to support the use of steel fibers extracted from waste tires in the production of concrete, with each study confirming the economic viability of using this material that is randomly distributed in nature.

In this regard, Moasa et al. [4] made clear that using steel fibers from used tires in concrete not only lessens pollution in the environment but also offers an opportunity for profitable engineering use. The management of waste tires, the application of steel fibers, and the longevity of both fresh and hardened fiber concrete were the main topics research review of Awolusi et al. [5]. According to research by Mohammad et al. [6], using waste tire steel fibers can reduce environmental degradation and enhance the fiber concrete's compressive strength and abrasion resistance.

Realizing the interest in using this material, many researchers have worked to define the good properties and characteristics of all the components of this composite material. Johnston [7] looked at the role of slenderness in flow and workability and considered that the fiber length should not exceed two times the nominal size of concrete to prevent fiber clumping and agglutination. This consideration was consolidated by Ulas et al. [8], who concluded that the aggregate grading and the Dmax have remarkable effects on the properties of fresh and hardened steel fiber-reinforced concrete

\*Corresponding author: Afif Rahma, Structure Department, Arab International University, Syria. Email: [a-rahma@aiu.edu.sy](mailto:a-rahma@aiu.edu.sy)

(FRC). Xia et al. [9] worked to define the relationship between steel fiber length and aggregate nominal size. Wang et al. [10] investigated the effects of steel fiber types and volume ratio on the physical and mechanical properties of concrete. The significant results of using steel fibers to improve the mechanical properties of concrete allowed Biswas et al. [11] to study the effects of steel fiber aspect and volume ratio on the fresh and harden properties of ultra-high-performance concrete, and they concluded that higher steel fiber aspect and volume ratio cause interlocking among fibers and improper distribution of fiber in concrete mixture, ultimately leading to reduce slump flow and decrease compressive strength. In view of these opposing effects due to the physical characteristics of fiber, Al-Hussaini et al. [12] as well as Sandoval-Siesquen and Muñoz-Pérez [13] advised using a valuable amount of plasticizers to address concrete consistency and ensure good workability.

In addition to the interest in the physical and mechanical aspects, numerous researchers have focused on the behavior of steel fiber concrete under different types of loads. Bernard [14] in his recent study justified the feasibility of using steel fiber to improve the mechanical properties of plain concrete. Başsürütçü et al. [15] studied the fiber type, shape, and volume ratio of the mechanical and flexural properties of concrete. Bayraktar et al. [16] proved that incorporating steel fibers greatly improves the splitting tensile strength and flexural strength of concrete and increases flexure toughness and post-cracking toughness. El-kassas et al. [17] worked on proportioning steel fiber concrete for pavement. Raj and Kumar [18] studied the effects of wires on the compressive strength of concrete to find out the optimum volume ratio of fiber in which the FRC gets more effective in terms of strength and crack resistance capacity. Above all, to ensure the durability of ground slab, Kos et al. [19] justified the use of steel fiber for strength, frost resistance, and resistance to acid attacks on steel FRC for industrial floors and road pavements.

Among these works, researchers have focused on the use of fibers extracted from tires for ground slabs. Graeff [20] looked at the long-term performance of steel fiber concrete; she proved that using steel fibers can improve the mechanical properties of plain concrete, which leads to the reduction of pavement depth; besides, she considered that the design codes for road pavements do not take into account the post-cracking behavior of steel fiber concrete and the fatigue criteria. Cakir and Cetisli [21] investigated the importance of the affecting parameters on the pressure-displacement relationship of steel FRC panels. Belletti et al. [22] worked on the effect of ductility on the load-carrying capacity of steel fiber concrete for ground slabs. Cajka et al. [23] studied the behavior of steel fiber concrete slabs under static loads, while Tekleab and Wondimu [24] looked at the effect of the impact load; furthermore, Achilleos et al. [25] worked on proportioning steel fiber concrete for pavement as well as their impact on the environment and cost. Smrkic et al. [26] justified the use of steel fiber to reduce the slab cracks caused by impact forces and dynamic loads applied to the concrete slab of roads and airstrips.

The ACI (5441. R-96) describes the suitable characteristics of steel fiber for concrete batches. Amin et al. [27] proposed a guidance for the appropriate composition and characteristics like length, diameter, and content of steel fiber in concrete applications including pavement.

Despite the material's advantages, Kooiman [28] in his research found that the consistency and workability of concrete are adversely affected by the random and inhomogeneous distribution of fiber. To overcome these defects, Zheng et al. [29] presented a novel dual-axis vibration mixing technology to address the shortcomings of random fiber distribution and enhance the performance

of ultra-high-performance concrete. At the modeling level, Löfgren et al. [30] worked on the stress transfer in fiber concrete and developed their parameter of stress distribution; moreover, Li et al. [31] proposed a probabilistic parameter to take into account the random distribution and the stochastic orientation of fibers in the concrete batch.

Besides the improvement of steel fiber that can bring to the mechanical properties of concrete, the issue that arises is what physical state must be taken into consideration to define the ductility limit and calculate the toughness of this composite material, taking into account the discontinuity and the physical destabilization of the hardened state of the concrete body observed during loading in the post-elastic stage; thus, this topic will be one of the goals of this work.

## 2. Research Interest

This research aimed to evaluate the profitability of utilizing steel fibers extracted from waste tires for the production of fiber concrete for the concrete ground slab. The study is distinguished from other works by its treatment of two distinct aspects. The first aspect is the consideration of the number of fibers as a parameter independent of the physical characteristics of the fibers and their volumetric rate; the second is the analysis of ductility and toughness, taking into account the discontinuity and the physical destabilization of the sample's state observed during the loading in the post-elastic stage.

## 3. Materials and Methods

### 3.1. Steel fiber

The steel wires were extracted from the beads of worn tires by splitting them from rubber (Figure 1(a) and Figure 1(b)), and then they were placed in an anaerobic oven at 180 °C for enough time until the residues turned into soot from the coal.

After extraction and cleaning, ten fiber samples were considered for testing where their diameter was 8 mm. These fibers were subsequently subjected to the tension test where the statistical analysis of the results gave an average of the elastic limit of the order of 1875 114 MPa, which is in agreement with the recommendation of the American Society for Testing and Materials (ASTM A A820-96) where the tensile strength is greater than 345 MPa.

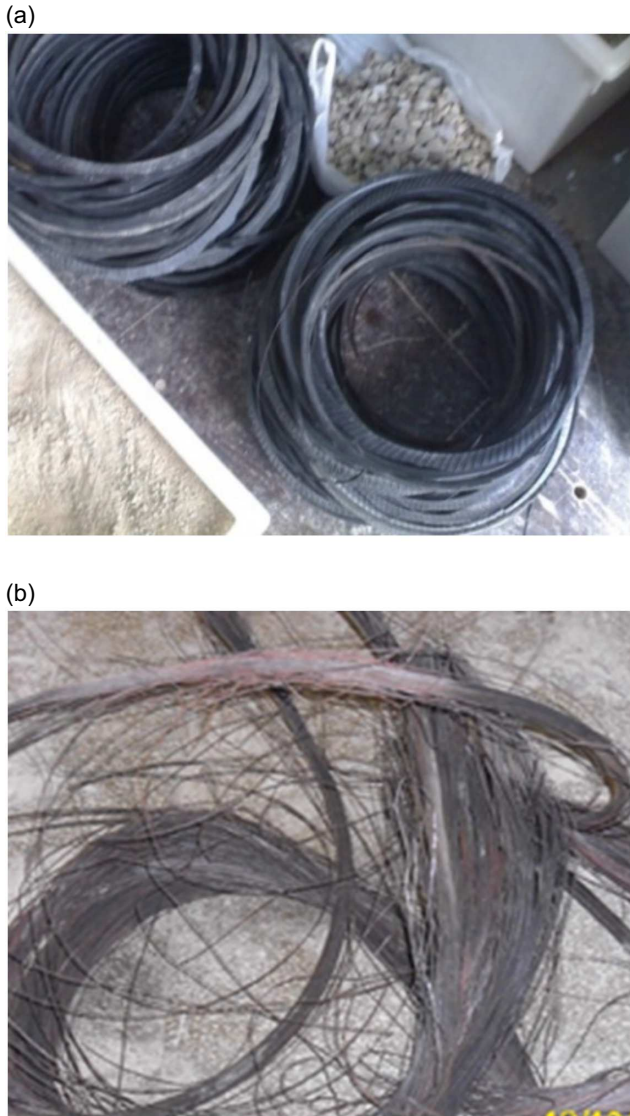
For the concrete batches, the wires were cut into 30, 40, and 60 mm length and placed in the Los Angeles Abrasion drum with a quantity of natural dune sand to mechanically remove the residual soot.

### 3.2. Concrete consistency

For the trial concrete mix design, three factors were taken into account: the length, the volume ratio of the steel fiber, and the number of fibers, which could affect the workability and increase the percentage of voids. Thus, to ensure a similar consistency for all batches (with and without fibers), a chemical additive type G (high range of water-reducing and retarding admixtures) was added in an appropriate quantity which varied from 1.2 to 2.4 kg per 100 kg of cement as needed; hence, the slump varied between 100 and 120 mm.

### 3.3. Concrete batches

According to ACI 318 and ACI 544.3R-93, concrete batches of 19 mm aggregate nominal size were designed for 300, 350, and

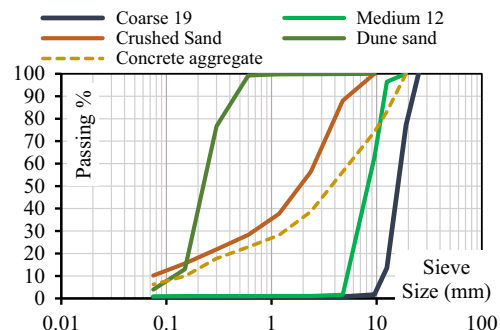
**Figure 1****(a) Bead wires. (b) Steel bead wires**

400 kg/m<sup>3</sup> cement type II (42.5 MPa). In order to guarantee a reliable analysis, concrete samples in cubic and cylindrical forms were prepared for fiber concrete and plain concrete, which served as a control sample. The steel fibers were added to the concrete with volume ratios of 0.5%, 1%, and 1.5%, respectively, 39.25, 78.5, and

117 kg/m<sup>3</sup>. Table 1 gives data regarding all information about the steel fibers, in addition to their numbers for each batch.

### 3.4. Aggregate sieve analysis

Locally, four types of aggregates are used (28% coarse, 20% medium, 48% crushed sand, and 7% dune sand to correct the fineness of the concrete aggregate). Figure 2 shows the aggregate curves with the aggregate composition of concrete aggregate.

**Figure 2****Grading diagram of component aggregates**

## 4. Results and Discussion

### 4.1. Compression test

To reveal the effect of the steel fiber on the concrete compression strength, tests were carried out gradually in two ways: the first ones concerned the amount of cement for 300, 350, and 400 kg/m<sup>3</sup> with fibers of 40 mm in length and a volume ratio of 0.5%, 1%, and 1.5%. The second step concerned the length of the fibers for 350 kg of cement with fibers of 30, 40, and 60 mm in length for a volume ratio of 1%. The results of the compression test ( $\sigma$ ) are shown in Figures 3–6.

Besides, the compression test shows two types of failure, where plain concrete takes the form of a pyramid, while the samples of fiber concrete have maintained their cubic shape (Figure 7).

The preliminary analysis of the behavior of fiber concrete, shown in Figures 3–6, allows drawing some notes summarized as follows: on the one hand, fiber concrete shows a significant increase in plastic deformation and ductility; on the other hand, it is evident that there is an irregularity in the collapse point. This crucial aspect requires a thorough examination of the effect of length, volumetric

**Table 1**  
**Characteristics data of the smooth waste steel fibers**

Diameter d (mm)	Length L <sub>f</sub> (mm)	Slenderness d/L <sub>f</sub>	volume ratio R <sub>v</sub> %		
			0.5%	1.0%	1.5%
Weight of fibers (kg) per 1 m <sup>3</sup> concrete					
0.8	30	37.5	331573	663146	994718
Numbers of fibers per 1 m <sup>3</sup> concrete					
0.8	40	50	248680	497359	746039
0.8	60	75	165786	331573	497359

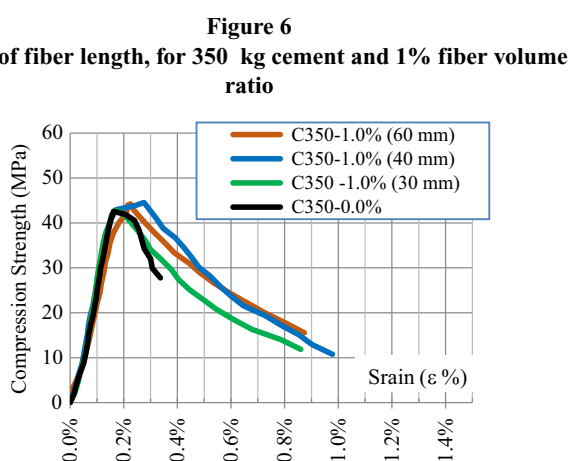
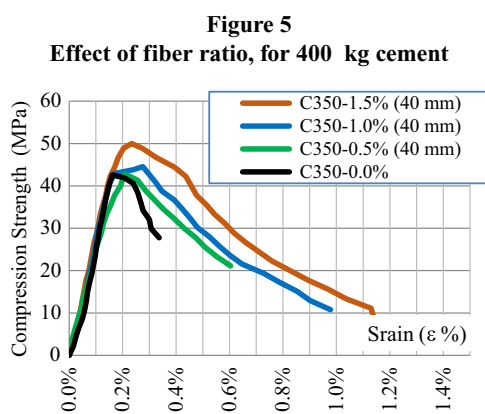
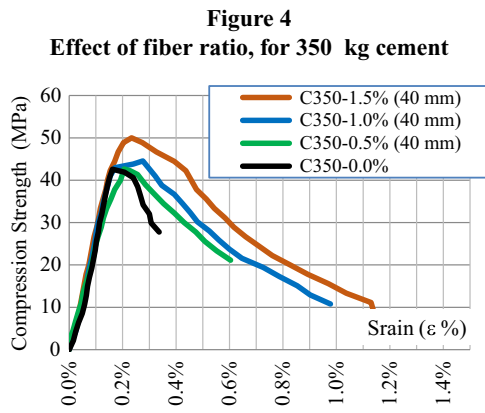
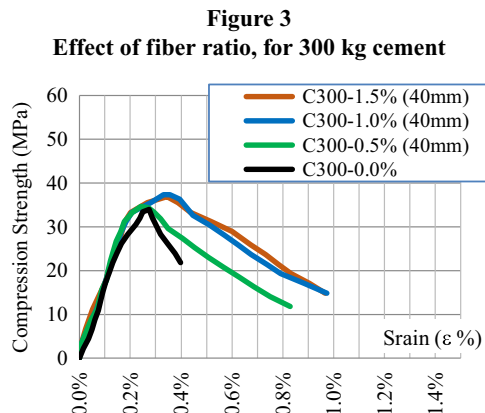
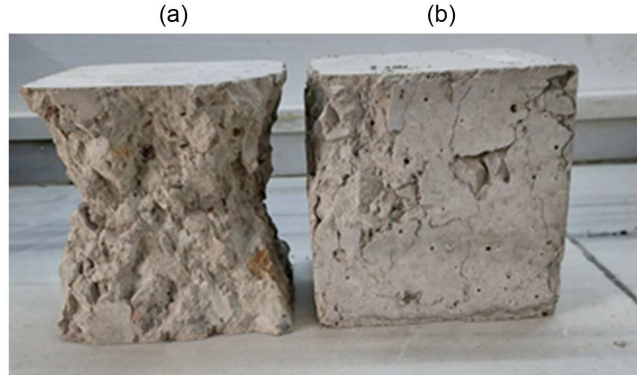


**Figure 7**  
(a) Plain concrete, (b) fiber concrete



ratio, and the interlocking of fibers on the physical structure of fiber concrete, which will be treated in detail below.

#### 4.2. Role of concrete components

As previously stated, the improvement in concrete strength is dependent on the quantity of cement and the fiber volume ratio. The linear regression (Figure 8) depicts the correlation between fiber concrete strength and fiber volume ratio, which can be elucidated by a straightforward linear relation of the form:

$$\sigma = \sigma_o + a.R_v \quad (1)$$

where  $(\sigma)$  is the strength value of fiber concrete,  $(\sigma_o)$  is the strength of plain concrete,  $(R_v)$  is the fiber volume ratio, and  $(a)$  is a constant that indicates the rate of gain associated with the amount of cement.

However, for a given length and volume ratio, the strength of fiber concrete shows significant improvement for 350 and 400 kg of cement, unlike the case of 300 kg cement, which shows low improvement in strength. For a first consideration, this result could be explained by the degree of cohesion due to the low amount of cement.

Regarding the role of fiber length, Figure 9 gives an overview of the impact of fiber length on the compressive strength of a given quantity of cement. For a given volume ratio of fiber and amount of cement, the slenderness of the 40 mm is more pronounced than that of the 30 and 60 mm. In comparison, the 30 mm length fiber improves the strength of the concrete slowly, while the 60 mm

**Figure 8**  
Contribution of cement quantity to the compression strength of fiber concrete

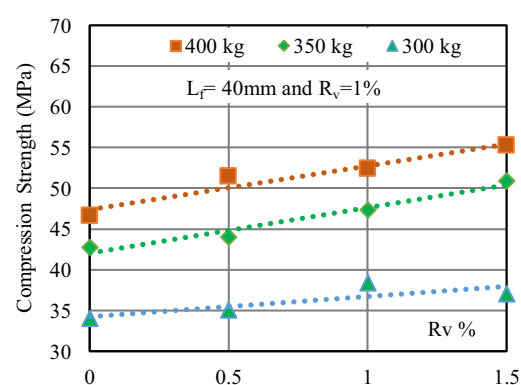
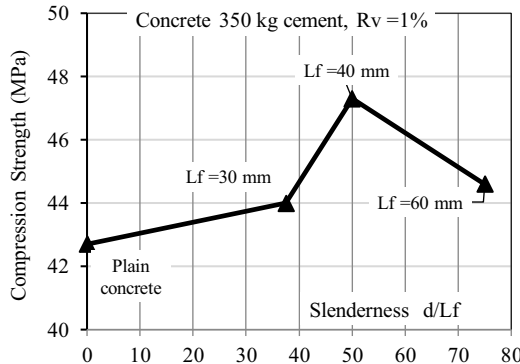


**Figure 9**  
Effect of fiber length on compression strength



length fiber considerably decreases the strength obtained compared to that of the 40 mm length fiber. These results lead to the conclusion that long fibers exceeding the nominal size of the concrete can cause an inconsistency in the fresh concrete and consequently affect and decrease the compressive strength of the hardened concrete.

#### 4.3. Influence of number of fibers

Considering the state of discontinuity and physical destabilization that the concrete samples undergo in the post-elastic state, the analysis of the effect of the number and size of fibers on the strength of fiber concrete was carried out for a strength limited to a strain of 0.2%.

Figure 10 shows that, for a given fiber length, the increase in  $R_v$  value (from 0.5% to 1.5% for a length of 40 mm) improves the strength of fiber concrete. Contrary to the previous result, Figure 11 demonstrates that for a given ratio of fiber volume, the increase in the number of fibers accompanied by a decrease in their size partially decreases the strength of this composite material. This phenomenon could be explained due to the random distribution of the fibers and the creation of voids where the fibers interlock.

Therefore, the concrete mix design must compromise between the length and number of fibers. Thus, it seems that for concrete with a 19 mm in nominal size, the most suitable is a volume ratio of 1% for a length of 40 mm.

**Figure 10**  
Effect of number of fibers on the compression strength

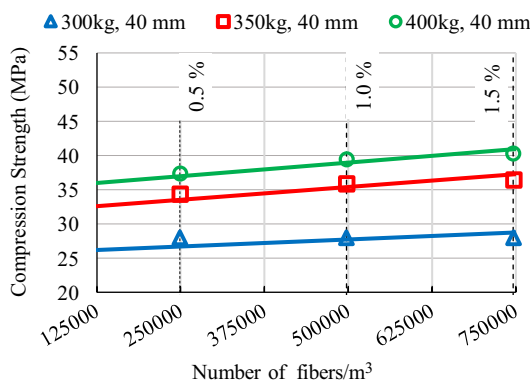
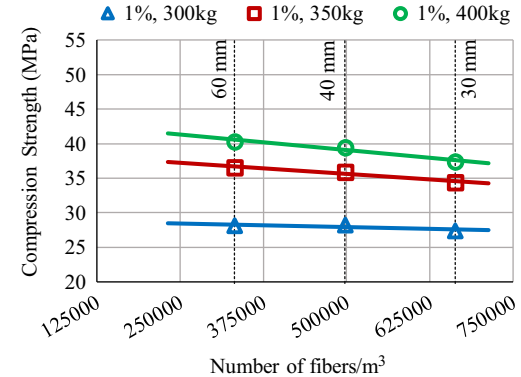


**Figure 11**  
Effect of fiber length on the compression strength



#### 4.4. Impact of fiber concrete ductility

As the curves ( $\sigma-\varepsilon$ ) in Figures 3–6 show, the first benefit of adding steel fiber is the wide ductility that concrete can gain. The failure of fiber concrete occurs at large deformation, and the failure of plain concrete occurs at a value of = 1.2–1.4%.

Following meticulously the process of the compression test, the physical state of the fiber concrete sample in the plastic deformation stage becomes physically discontinuous and destabilized, which partly explains the dispersed limit of the failure strain (Figures 3–6). This, in turn, describes the ductility of the material. In this case, it is difficult to determine the effective failure stage, contrary to plain concrete, which behaves as a brittle material (Figure 7).

It appears that the force-deformation that the device continues to provide is not due to the strength of the continuous material but to the cohesion and bond between the concrete fragments and the steel fibers.

#### 4.5. Toughness and toughness index

The ductility is expressed quantitatively by the toughness ( $T$ ) calculated by the surface area under the force-displacement curve and given by the formula:

$$T = fP.d\delta. \quad (2)$$

This integration quantifies the amount of energy dissipated to reach the failure state of the material, where  $P$  and  $d\delta$  are, respectively, the charge and the displacement.

For one cubic sample of ( $L$ ) side and ( $V$ ) volume of the cube, the dissipated energy, called volume toughness  $T_V$ , Formula (2) takes the form:

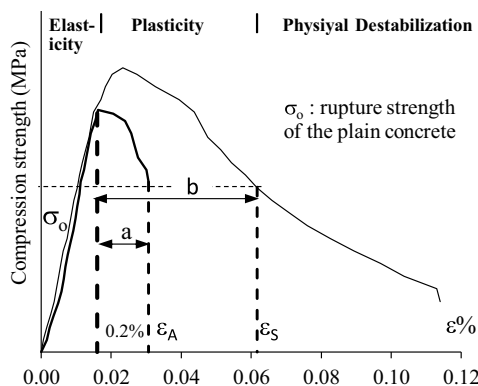
$$T_V = T/V = (1/V)fP.d\delta = f\sigma.d\varepsilon \quad (3)$$

With: the strength  $\sigma = P/A$ , and the strain  $d\varepsilon = d\delta/L$

Furthermore, the toughness index ( $T_I$ ) is given to show the difference between the ductility of two cases of concrete, like the fiber and plain concrete. It is given by the relationship  $T_I = T_B/T_A$ , where  $T_A$  and  $T_B$  are, respectively, the toughness of plain concrete and fiber concrete.

In this sense, the ductility of fiber concrete and its level prior to failure cannot be determined by a single criterion. Bayasi and Soroushian [32] calculated the ductility for a strain rate of 5.5 times that of the maximum strength, whereas Mansur et al. [33] restricted the strain to three times that of the maximum strength. Taerwe [34] suggested that the limit to be considered is a strain rate of

**Figure 12**  
The proposal method to calculate the toughness  $T$  and  
toughness index  $T_I = T_B/T_A$



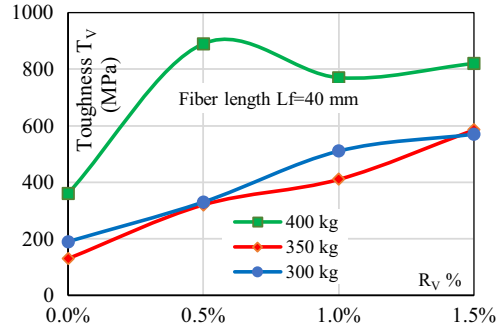
0.7%. According to recent research, Yang et al. [35] looked at the improvement of fiber concrete properties and estimate the increase of ductility by 98% in terms of energy. According to this study, the effective volume toughness of the fiber concrete was calculated for the ultimate deformation of the sample.

Unlike the previous considerations, this study adopts another way to measure the ductility and calculate the toughness of fiber concrete, where the plastic deformation is limited to the physical stability state of the concrete sample, as shown in Figure 12. Therefore, the ductility domain of the two cases corresponds to the failure strength ( $\sigma_0$ ) that matches the plastic strain ( $\epsilon_a$  and  $\epsilon_b$ ) of plain concrete and fiber concrete, respectively.

Therefore, the proposed volume toughness value given in Tables 2 and 3 is calculated by integrating the area under the curve ( $\sigma$ - $\epsilon$ ) between two limits: the strain of the elastic yield stress (defined conventionally at  $\epsilon = 0.2\%$ ) and the plastic strain ( $\epsilon_A$ ) for plain concrete and ( $\epsilon_S$ ) for the fiber concrete, corresponding, respectively, to the amount of the load failure ( $f$ ) of plain concrete.

Thus, the values of  $T_V$  and  $T_I$  are given in Table 2 and illustrated in Figures 13 and 14 for the fiber concrete of 300, 350, and 400 kg/m<sup>3</sup> cement and 40 mm fiber length. Moreover, Table 3, as illustrated in Figure 15, provides the values of  $T_V$  and  $T_I$  for the fiber concrete composed of 350 kg/m<sup>3</sup> cement with varying fiber lengths and a 1% fiber volume ratio.

**Figure 13**  
Effect of fiber volume ratio  $R_v$  on the toughness  $T_V$



Figures 13 and 14 show a significant correlation of  $T_V$  and  $T_I$  with the volume ratio  $R_v$  for concrete of 300 and 350 kg of cement. However, the contribution of steel fiber is limited to  $R_v = 0.5\%$  for concrete of 400 kg of cement. This raises the question of the relationship between  $R$  and the amount of cement, which deserves a more in-depth study.

On the other hand, the value of  $T_V$  and  $T_I$  for 300 kg of cement shows a certain tendency to be restricted after a value of  $R_v = 1.5\%$ . This result suggests that the effect of the fiber volume ratio is related to the characteristic properties of cement concrete and its moderate resistance.

The obvious role of  $R_v$  for 350 kg of cement allows looking at the effect of fiber length (L) on fiber concrete. Figures 15 and 16 illustrate the value of  $T_V$  and  $T_I$  for fiber concrete of 350 kg of cement, with  $R_v = 1\%$ . The curves indicate that the significant effect of fiber is limited to a length of 40 mm, which confirms the conclusion of previous researchers that the best fiber length is one that is equal to two times the nominal size of the concrete aggregate. Thus, for 19 mm concrete nominal aggregate, fibers could be limited to 40 mm length and a 1% volume ratio.

#### 4.6. Contribution of fiber to concrete strength

Admitting the random distribution of fibers in concrete mix [36], Löfgren et al. [30] considered that in a concrete mix with uniaxial orientation, the two parts of the fibers are statically equal on the two sides of the crack plan. Similarly, Stang and Li [37] introduced the fiber orientation factor ( $\eta_{\phi 3D} = 1/2$ ) within the three-

**Table 2**  
Values of toughness ( $T_V$ ) and toughness for 300, 350, and 400 kg cement and different fiber ratios

Cement weight (fiber length)	$R_v$	0	0.5%	1%	1.5%
300 kg (40 mm)	$T_V$ (MPa)	190	330	510	570
	$T_I$	1.00	1.74	2.68	3
	$\epsilon\%$	0.40%	0.54%	0.70%	0.78%
350 kg (40 mm)	$T_V$ (MPa)	130	320	410	585
	$T_I$	1.00	2.46	3.15	4.54
	$\epsilon\%$	0.33%	0.47%	0.53%	0.64%
400 kg (40 mm)	$T_V$ (MPa)	360	890	770	820
	$T_I$	1.00	2.47	2.14	2.28
	$\epsilon\%$	0.47%	0.72%	0.70%	0.71%

**Table 3**  
**Values of toughness (TV) and toughness index for 350 kg cement and different fiber lengths**

Length of fiber	0	30 mm	40 mm	60 mm
T <sub>V</sub> (MPa)	130	220	410	445
T <sub>I</sub>	1	1.7	3.15	3.40
ε%	0.33%	0.45%	0.53%	0.57%

**Figure 14**  
**Effect of fiber volume ratio R<sub>v</sub> on the toughness index T<sub>I</sub>**

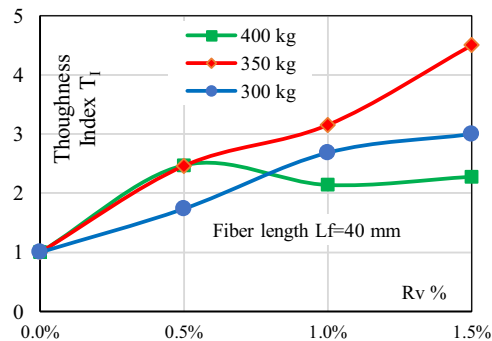


**Figure 15**  
**Effect of fiber length the toughness T<sub>V</sub>**

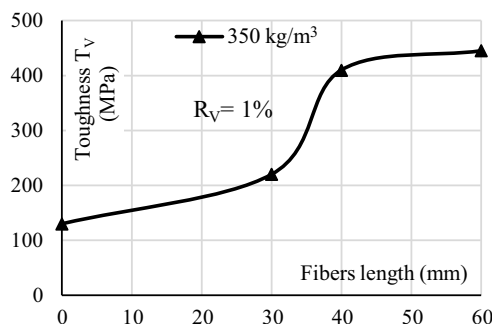
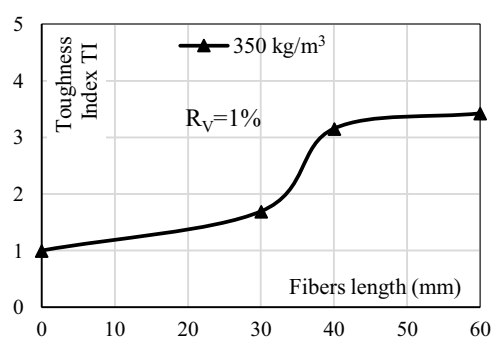
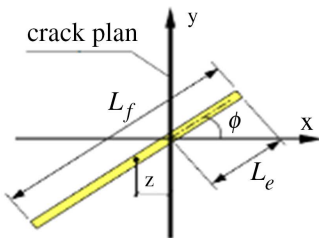


**Figure 16**  
**Effect of fiber length on the toughness index T<sub>I</sub>**



dimensional space (Figure 17 [37]). Its value is calculated by integrating the probability formula for the density function of two parameters  $p(z)$  and  $p(\Phi)$ , where  $(z)$  is the center of gravity of the fibers and  $(\Phi)$  is its orientation in space. Therefore,  $(\eta_\phi)$  assumes the form  $(\eta_{\phi 3D})$  and possesses the value  $\eta_{\phi 3D} = 1/2$ . Hence, the length of fiber dipped ( $L_e$ ) in the space is equal to  $1/4$  of the fiber's length ( $L_f$ ).

**Figure 17**  
**Random distribution of fiber**



Considering these factors, the contribution of fiber is derived from the equation of equilibrium forces:

$$F_m = F_f + F_c \quad (4)$$

where in  $F_m$ ,  $F_f$ , and  $F_c$  represent, respectively, the proportion of applied force across the entire section, the proportion of force on the fibers, and the proportion of force on the concrete.

This equality is developed as follows:

$$A_m \cdot \sigma_m = \eta_{\phi 3D} \cdot A_f \cdot \sigma_f + A_c \cdot \sigma_c \quad (5)$$

$$\sigma_m = \eta_{\phi 3D} \cdot (A_f / A_m) \cdot \sigma_f + A_c / A_m \cdot \sigma_c \quad (6)$$

$$\sigma_m = \eta_{\phi 3D} \cdot (R_v / 2) \cdot \sigma_f + (1 - \eta_{\phi 3D} \cdot R_v) \cdot \sigma_c \quad (7)$$

$$\sigma_m = (R_v / 2) \cdot \sigma_f + (1 + (R_v / 2)) \cdot \sigma_c \quad (8)$$

$$\sigma_m = (R_v / 2) \cdot \sigma_f [\sigma_f - (1 + (R_v / 2)) \cdot \sigma_c] \quad (9)$$

And  $A_m$ ,  $A_f$ , and  $A_c$  are, respectively, the total cross-section area of the sample, the equivalent cross-section area of the fibers, and the cross-section area of the concrete.  $\sigma_f$ , and  $\sigma_c$  are, respectively, the maximum compression stress on the section area, the compression stress portion of fibers, and the compression stress portion of the concrete.

$\sigma_m$ ,  $\sigma_f$ , and  $\sigma_c$  are, respectively, the maximum compression stress on the section area, the compression stress portion of fibers, and the compression stress portion of the concrete.

Figures 18 and 19 demonstrate that the impact of the steel fibers on all concrete batches is contingent upon the concrete characteristics, the volume ratio of steel fiber, and the fiber length. However, the contribution of fiber decreases gradually with increasing its volume ratio, regardless of the amount of cement. The length of the fiber also loses its role after a certain length, here 40 mm in length. This conclusion is consistent and aligns well with what was presented previously.

**Figure 18**  
Effect of volume fiber ratio on compression strength

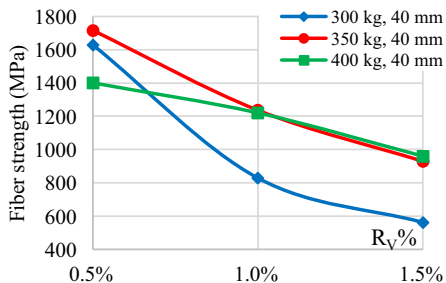
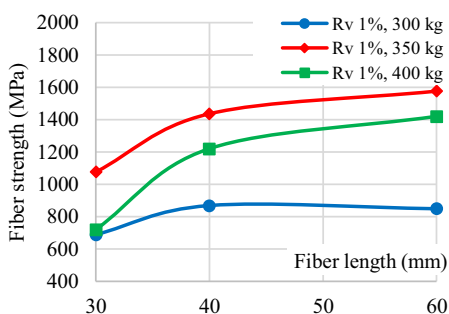


**Figure 19**  
Effect of volume fiber ratio on compression strength



#### 4.7. Tension and spilling test

The behavior of ground slabs is characterized by the interaction between the externally applied loads and the elastic soil reaction, as well as the internal alternation of tension and compression stresses. Thus, after acquiring knowledge of the contribution of steel fibers under compression, it is necessary to study closely the behavior of this composite material under tensile load to fully understand the role of the fibers in this case of alternating resistance.

On the basis of the previous results of concrete for 350 kg of cement, spilling and flexure tests were carried out using the same batches with steel fiber of 40 mm length and a 1% volume ratio. In addition to studying the effect of the number of fibers, three samples for each test were made for concrete with fiber for a length of 60 mm and a volume ratio of 1.5%, thus ensuring the same number of fibers as shown in Table 1. For correct comparison, the applied charges were registered systematically just for a crack of the order of 0.1 mm.

##### 4.7.1. Spilling tension test

Three specimens of standard cylinders were utilized for each of the plain concrete and fiber concrete, as depicted in Figure 20. The average value of the splitting stress ( $f_c$ ) of plain concrete and fiber concrete ( $f_{sm}$ ) shows that the steel fiber improves approximately 2.5 times the spilling tension strength of plain concrete (Figure 21).

##### 4.7.2. Flexure tension test

To evaluate the flexure tension strength ( $f_t$ ) and avoid the effect of shear stress, the four-point bending test was applied for a 30 cm bending span (Figure 22). The average tension stresses for both cases with and without fiber were calculated simply by utilizing the equation  $\sigma = M.y/I$ .

Taking into consideration that at the first crack of the beam, the applied elastic stress will be transmitted gradually and linearly to

**Figure 20**  
Samples of splitting test



**Figure 21**  
Spilling strength for plain and fiber concrete

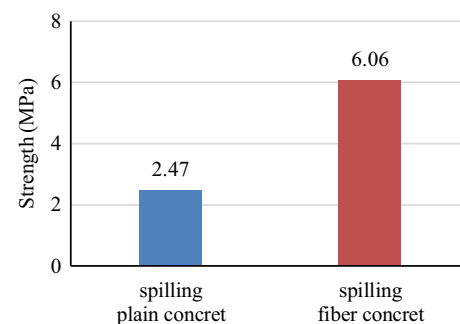


**Figure 22**  
Samples of flexure test



the steel fiber. The CEB-FIB considers that the moderate value of the tension stress on the steel fiber ( $f_{ts}$ ) could be reduced by 40%. The results in Figure 23 demonstrate that the value of the flexure strength for plain concrete matches well with that of spilling strength (Figure 21), where the steel fiber increases the strength of concrete from 1.98 MPa for plain concrete to 6.56 MPa and improves approximately three times the flexure tension strength of plain concrete. Therefore, this value was taken below as a moderate value to calculate the cohesion stress between the concrete and fiber.

#### 4.8. Cohesive stress between fiber and concrete

By utilizing the previous Equations (4)–(9) and considering the reduced tension stress applied to the hypothetical steel fiber located on the external side of the beam, as outlined below, the average

**Figure 23**  
**Flexure strength for plain and fiber concrete**

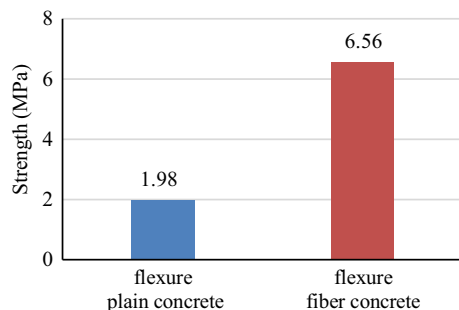


**Figure 24**  
**Tensile strength attributed to fibers**

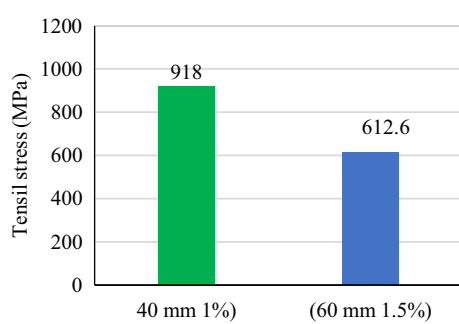
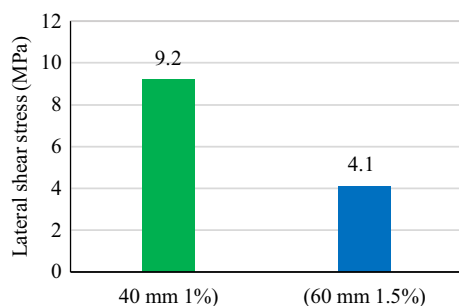


**Figure 25**  
**Lateral shear strength attributed to fibers**



tensile stress between the concrete and fiber is determined by utilizing the following formula:

$$f_f = (2/R_v)[f_c - (1 - (R_v/2)f_m)] \quad (10)$$

This hypothetical value reaches a value of 918 MPa, which is still below the specific strength of 1875 MPa of fiber. Thus, the shear stress  $\tau_s$  between steel fiber and concrete is calculated from the equilibrium of forces, the result of lateral shear and tension stresses given by the formula:

$$f_f(\pi \cdot d^2/4) = \tau \cdot 2\pi \cdot d \cdot L_{\phi 3d} = \tau \cdot 2\pi \cdot d \cdot (L_f/4) \quad (11)$$

Figures 24 and 25 show, respectively, the contribution of fiber under spalling and flexure loads for a fiber of 40 mm length and 1% volume ratio.

To determine the effect of the number density of fibers on the behavior of hardened concrete, tension and lateral shear stresses

were calculated for the same number of fibers in concrete batches. The comparison was made between concrete with fiber of 4 mm length and 1% volume ratio and concrete with fiber of 6 mm length and 1% volume ratio, where concrete batches have the same number of fibers as shown in paragraph (4.7). The results shown in Figure 23 indicate that the tensile stress ( $f_f$ ) decreases from 918 MPa for fibers of 40 mm to 612.6 MPa for fibers of 60 mm. The same is for shear stress ( $\tau_s$ ) shown in Figure 24, where stress decreases from 9.2 MPa for fibers of 40 mm to 4.1 MPa for 60 mm in length.

Thus, the values of ( $f_f$ ) and ( $f_s$ ) for the same number of fibers prove that a fiber of 40 mm is more efficient than that of 60 mm, although the volume ratio in the latter case is greater. This phenomenon could be explained by the bad effect of interlocking, and the appropriate fiber for aggregate concrete of 19 mm nominal size is a fiber of 40 mm length with a 1% volume ratio.

## 5. Conclusions

This study proposes a new method for calculating the effective ductility range and toughness of hardened FRC. This method takes into account the discontinuity, physical destabilization of hardened concrete, and the behavior of FRC after the elastic phase, where these factors partly explain the irregularity of plastic behavior and scattered strain value at failure.

The experimental outcomes demonstrate the viability of investing and utilizing the steel fibers extracted from waste wires to enhance the mechanical properties of concrete under compression, splitting, and flexure loads at the elastic and plastic domains.

The effect of steel fiber on compression appears to be modest and does not increase the strength of fiber concrete, but they have the capacity and performance to significantly increase the ductility and toughness of concrete at the plastic stage. This acquired property can be attributed to the role of fiber that delays failure up to a strain of the order of 1.2–1.4%, while it occurs for 0.3–0.4% strain in the case of ordinary concrete. Thus, steel fiber increases the toughness index by two to four times compared to ordinary concrete.

Contrary to compression charge, the study demonstrates that the inclusion of steel fiber in concrete enhances the splitting and flexural stresses and increases strength by more than three times that of plain concrete.

In general, the study indicates that the performance of the fiber concrete for any amount of cement depends on the length and the slenderness, as well as the volume ratio of the fibers. However, it is imperative to consider the interlocking between fibers, which may affect the mechanical properties of concrete. It appears that the best performance of 19 mm nominal size of aggregate concrete can be formulated with a fiber of 40 mm length and a 1% volume ratio.

## Ethical Statement

This study does not contain any studies with human or animal subjects performed by the author.

## Conflicts of Interest

The author declares that he has no conflicts of interest to this work.

## Data Availability Statement

Data are available from the corresponding author upon reasonable request.

## Author Contribution Statement

**Afif Rahma:** Conceptualization, Methodology, Formal analysis, Investigation, Resources, Data curation, Writing – original draft, Writing – review & editing, Visualization, Supervision, Project administration.

## References

[1] Lagarinhos, C., Espinosa, D., Tenório, J., & de Azevedo, L. (2023). The management of waste tires. In M. Vithanage & M. N. V. Prasad (Eds.), *Microplastics in the ecosphere: Air, water, soil, and food*. Wiley. <https://doi.org/10.1002/9781119879534.ch30>

[2] Šourková, M., & Adamcová, D. (2023). Establishing impact of the long-term action of waste dumps with the occurrence of waste tires on the soil environment. *Polish Journal of Environmental Studies*, 32(4), 3787–3798. <https://doi.org/10.15244/pjoes/163567>

[3] Czarna-Juszkiewicz, D., Kunecki, P., Cader, J., & Wdowin, M. (2023). Review in waste tire management-Potential applications in mitigating environmental pollution. *Materials*, 16(17), 5771. <https://doi.org/10.3390/ma16175771>

[4] Moasa, A. M., Amin, N., Khan, K., Ahmad, W., Al-Hashem, M. N. A., Deifalla, A. F., ..., & Ahmad, A. (2022). A worldwide development in the accumulation of waste tires and its utilization in concrete as a sustainable construction material: A review. *Case Studies in Construction Materials*, 17, e01677. <https://doi.org/10.1016/j.cscm.2022.e01677>

[5] Awolusi, T. F., Oke, O. L., Atoyebi, O. D., Akinkurolere, O. O., & Sojobi, A. O. (2021). Waste tires steel fiber in concrete: A review. *Innovative Infrastructure Solutions*, 6, 34. <https://doi.org/10.1007/s41062-020-00393-w>

[6] Mohammad, S. A., Krishna, T. N. C., Saketh, T., Ganesh, C. Y., & Sathyam, D. (2023). Fresh and hardened state properties of waste tire fiber and steel fiber reinforced concrete. *Materials Today: Proceedings*, 80, 443–448. <https://doi.org/10.1016/j.matpr.2022.10.195>

[7] Johnston, C. D. (2014). *Fiber-reinforced cements and concretes*. UK: Taylor & Francis.

[8] Ulas, M. A., Alyamaç, K. E., & Ulucan, Z. C. (2017). Effects of aggregate grading on the properties of steel fibre-reinforced concrete. *IOP Conference Series: Materials Science and Engineering*, 246, 012015. <https://doi.org/10.1088/1757-899X/246/1/012015>

[9] Xia, D., Xie, S., Fu, M., & Zhu, F. (2021). Effects of maximum particle size of coarse aggregates and steel fiber contents on the mechanical properties and impact resistance of recycled aggregate concrete. *Advances in Structural Engineering*, 24(13), 3085–3098. <https://doi.org/10.1177/13694332211017998>

[10] Wang, Z., Li, H., Zhang, X., Chang, Y., Wang, Y., Wu, L., & Fan, H. (2023). The effects of steel fiber types and volume fraction on the physical and mechanical properties of concrete. *Coatings*, 13(6), 978. <https://doi.org/10.3390/coatings13060978>

[11] Biswas, R. K., Bin Ahmed, F., Ehsanul Haque, M., Provasha, A. A., Hasan, Z., Hayat, F., & Sen, D. (2021). Effects of steel fiber percentage and aspect ratios on fresh and hardened properties of ultra-high performance fiber reinforced concrete. *Applied Mechanics*, 2(3), 501–515. <https://doi.org/10.3390/applmech2030028>

[12] Al-Hussaini, O. M., AL-Baghdadi, W. H., Al-Labban, S. N., & Jabal, Q. A. (2020). Investigation the properties of waste plastic fiber concrete modified with HP-570 super-plasticizer. *IOP Conference Series: Materials Science and Engineering*, 978, 012026. <https://doi.org/10.1088/1757-899X/978/1/012026>

[13] Sandoval-Siesquen, F. E., & Muñoz-Pérez, S. P. (2025). Efectos de la incorporación de fibras de acero con aditivo plastificante en el hormigón [Effects of incorporating steel fibers with a plasticizing additive in concrete]. *Revista Facultad de Ingeniería Universidad de Antioquia*, (115), 84–94. <https://doi.org/10.17533/udea.redin.20240515>

[14] Bernard, E. S. (2023). Long-term post-crack performance of high-strength fiber-reinforced concrete for structural applications. *Structural Concrete*, 24(1), 1134–1151. <https://doi.org/10.1002/suco.202100740>

[15] Başsürütü, M., Fenerli, C., Kına, C., & Akbaş, S. D. (2022). Effect of fiber type, shape and volume fraction on mechanical and flexural properties of concrete. *Journal of Sustainable Construction Materials and Technologies*, 7(3), 158–171.

[16] Bayraktar, O. Y., Kapla, G., Shi, J., Benli, A., Bodur, B., & Turkoglu, M. (2023). The effect of steel fiber aspect-ratio and content on the fresh, flexural, and mechanical performance of concrete made with recycled fine aggregate. *Construction and Building Materials*, 368, 130497. <https://doi.org/10.1016/j.conbuildmat.2023.130497>

[17] El-kassas, A. I., Bashandy, A. A., Eied, F. A. M., & Arab, M. A. E. S. (2022). Effect of fibers type on the behavior of fibrous high-strength self-compacted reinforced concrete flat slabs in punching with and without shear reinforcement. *Construction and Building Materials*, 360, 129625. <https://doi.org/10.1016/j.conbuildmat.2022.129625>

[18] Raj, S., & Kumar, R. (2024). Analysis the strength of concrete using steel fibre reinforced. *Journal of Civil Engineering Research & Technology*, 6(5), 1–7. [https://doi.org/10.47363/JCERT/2024\(6\)164](https://doi.org/10.47363/JCERT/2024(6)164)

[19] Kos, Z., Krovíakov, S., Kryzhanovskyi, V., & Hedulian, D. (2022). Strength, frost resistance, and resistance to acid attacks on fiber-reinforced concrete for industrial floors and road pavements with steel and polypropylene fibers. *Materials*, 15(23), 8339. <https://doi.org/10.3390/ma15238339>

[20] Graeff, A. G. (2011). *Long-term performance of recycled steel fiber reinforced concrete for pavement applications*. PhD Thesis, University of Sheffield.

[21] Cakir, O. E., & Cetisli, F. (2022). Behavior of steel fiber reinforced concrete panels under surface pressure. *Sustainability*, 14(1), 298. <https://doi.org/10.3390/su14010298>

[22] Belletti, B., Cerioni, R., Meda, A., & Plizzari, G. (2008). Design aspects on steel fiber-reinforced concrete pavements. *Journal of Materials in Civil Engineering*, 20(9), 599–607.

[23] Cajka, R., Marcalikova, Z., Kozielova, M., Mateckova, P., & Sucharda, O. (2020). Experiments on fiber concrete foundation slabs in interaction with the subsoil. *Sustainability*, 12(9), 3939. <https://doi.org/10.3390/su12093939>

[24] Tekleab, E., & Wondimu, T. (2022). Behavior of steel-fiber-reinforced concrete (SFRC) slab-on-grade under impact loading. *Advances in Civil Engineering*, 2022(1), 6232757. <https://doi.org/10.1155/2022/6232757>

[25] Achilleos, C., Hadjimitsis, D., Neocleous, K., Pilakoutas, K., Neophytou, P. O., & Kallis, S. (2011). Proportioning of steel fiber reinforced concrete mixes for pavement construction and their impact on environment and cost. *Sustainability*, 3(7), 965–983. <https://doi.org/10.3390/su3070965>

[26] Smrkic, M. F., Damjanovic, D., Baricic, A., & Uroš, M. (2022). Experimental and numerical analysis of concrete slabs

reinforced with rebar and recycled steel fibers from waste car tyres. *Structural Concrete*, 24(2), 1807–1820. <https://doi.org/10.1002/suco.202200640>

[27] Amin, M. N., Khan, K., Nazar, S., & Deifalla, A. F. (2023). Application of waste recycle tire steel fibers as a construction material in concrete. *Reviews on Advanced Materials Science*, 62(1), 20220319. <https://doi.org/10.1515/rams-2022-0319>

[28] Kooiman, A. G. (2000). *Modelling steel fiber reinforced concrete for structural design*. PhD Thesis, Technische Universiteit Delft.

[29] Zheng, Y., Zhou, Y., Nie, F., Luo, H., & Huang, X. (2022). Effect of a novel vibration mixing on the fiber distribution and mechanical properties of ultra-high performance concrete. *Sustainability*, 14(13), 7920. <https://doi.org/10.3390/su14137920>

[30] Löfgren, I., Stang, H., & Olesen, J. F. (2005). Fracture properties of FRC determined through inverse analysis of wedge splitting and three-point bending tests. *Journal of Advanced Concrete Technology*, 3(3), 423–434. <https://doi.org/10.3151/jact.3.423>

[31] Li, Z., Wu, M., Wu, J., Cui, Y., & Xue, X. (2020). Steel fibre reinforced concrete meso-scale numerical analysis. *Advances in Civil Engineering*, 2020(1), 2084646. <https://doi.org/10.1155/2020/2084646>

[32] Bayasi, Z., & Soroushian, P. (1989). Optimum use of pozzolanic materials in steel fiber reinforced concrete. *Transportation Research Record*, 1226, 25–30.

[33] Mansur, M. A., Chin, M. S., & Wee, T. H. (1997). Stress–strain relationship of confined high strength plain and fiber concrete. *Journal of Materials in Civil Engineering*, 9(4), 171–178. [https://doi.org/10.1061/\(ASCE\)0899-1561\(1997\)9:4\(171\)](https://doi.org/10.1061/(ASCE)0899-1561(1997)9:4(171))

[34] Taerwe, L. R. (1993). Influence of steel fibers on strain-softening of high-strength concrete. *Materials Journal*, 89(1), 54–60. <https://doi.org/10.14359/1245>

[35] Yang, I., Park, J., Bui, T., Kim, K., Joh, C., & Lee, H. (2020). An experimental study on the ductility and flexural toughness of ultrahigh-performance concrete beams subjected to bending. *Materials*, 13(10), 2225. <https://doi.org/10.3390/ma13102225>

[36] Raju, R. A., Lim, S., Akiyama, M., & Kageyama, T. (2020). Effects of concrete flow on the distribution and orientation of fibers and flexural behavior of steel fiber-reinforced self-compacting concrete beams. *Construction and Building Materials*, 262, 119963. <https://doi.org/10.1016/j.conbuildmat.2020.119963>

[37] Stang, H., & Li, V. C. (2004). Classification of fiber reinforced cementitious materials for structural applications. In *Proceedings of the Sixth International RILEM Symposium*, 197–218.

**How to Cite:** Rahma, A. (2026). Investigating the Steel Fiber of Waste Tires to Enhance the Properties of Concrete Ground Slabs. *Archives of Advanced Engineering Science*, 4(1), 102–112. <https://doi.org/10.47852/bonviewAAES52025040>